Nonequilibrium Characteristics of Nitrogen Plasmas Appropriate to an AOTV Flight

By

Hiroyuki SHIRAI*

(February 5, 1987)

Summary: Nonequilibrium electronic excitations and deexcitations in nitrogen plasmas appropriate to an AOTV flight are studied theoretically. From the given nonequilibrium thermodynamic state variables behind a strong shock wave, the number densities of internal states of a nitrogen atom, nitrogen molecule and nitrogen ionic molecule are calculated by using the collisional and radiative process theory, in which the effects of heavy particle impacts are included. Based on the results of the nonequilibrium population distributions at various electronic states of each species, emission and absorption characteristics of the plasmas are calculated.

1. INTRODUCTION

It is well known that an AOTV is designed, because of its intrinsic requirements and constraints, to fly in the high-altitide and low density region of Earth's atmosphere at a nearescape velocity [1]. In such an environment, the shock layer around the vehicle can produce significant radiation [2]. Since the radiation will be surely enhanced by chemical and thermal nonequilibrium, one must be able to calculate the radiative heat fluxes to the vehicle based on nonequilibrium theory to provide a heat-shield design with confidence.

The purpose of the present paper is to examine closely nonequilibrium state of nitrogen plasmas appropriate to such an AOTV flight. Nonequilibrium population distributions at excited electronic states of atomic and molecular species, which are related directly to the radiative properties of the plasmas, are calculated by using the theory of collisional and radiative processes [3], and absorption coefficient and emittance of the plasmas are derived from the population distributions.

2. COLLISIONAL AND RADIATIVE PROCESSES

To evaluate nonequilibrium radiation from plasmas, populations of excited levels of atoms and molecules from which radiation emanates must be known. If macroscopic plasma parameters such as various temperatures, electron density, and total population of each species in interest are given, such populations can be calculated based on the collisional-radiative process theory by Bates, *et al.* [3].

According to this process theory, a collision by an electron or a heavy particle can cause a transition of electronic state of the target atom or molecule from an initial

* Faculty of Engineering, Gunma University.

lower state i to final upper state j at the rate

$$K_{ij}n_c n_i, \tag{1}$$

if the relative collision energy exceeds the energy difference between the two states $E_{ex}=E_j-E_i$. The excitation rate coefficient K_{ij} is basically expressed as

$$K_{ij}=\int_{E_{ex}}^{\infty} F(E)v(E)Q_{ij}(E)dE. \tag{2}$$

In the above expressions, n_c is the number density of the colliding species, n_i that of the initial state, E the relative collision energy, $F(E)$ the distribution of the collision energy, $v(E)$ the relative velocity between the two colliding species, and Q_{ij} the collision cross section for the transition. The rate of deexcitation from higher excited states to lower ones is related to the excitation rate by the principle of detailed balance.

The production rate of the state i including radiative transitions is given by

$$\sum_{j=1}^{\infty}(K_{ji}n_c+A_{ji})n_j, \tag{3}$$

where A_{ji} is the radiative transition probability from the state j to i. In a similar manner, the removal rate of the state i is given by

$$\sum_{j=1}^{\infty}(K_{ij}n_c+A_{ij})n_i. \tag{4}$$

These rates are known to be usually much larger in magnitude than the other rates such as diffusion rates of heavy particles and the rate of change of macroscopic plasma parameters encountered in high-temperature flows like an AOTV flight. As a result, the number density of the state n_i can be assumed to be in the local steady state, and one obtains the following quasi-steady-state relation,

$$\sum_{j=1}^{\infty}(K_{ji}n_c+A_{ji})n_j-\sum_{j=1}^{\infty}(K_{ij}n_c+A_{ij})n_i=0. \tag{5}$$

This equation forms a set of linear equations for n_j's and the solution is obtainable by the algebraic operations.

The collision cross section data Q_{ij} are needed to calculate Eq. (2) and hence Eq. (5) for many transitions. Those for election impact excitations are generally available from many theoretical and experimental studies. However, there are few data on the excitation cross sections by heavy particle impacts.

3. Collisional Transition Rates

To carry out the computation, one needs modeling for energy-state structures of atoms and molecules, because they are too complex to be handled as they are. For a nitrogen atom, the same energy-state grouping as in Ref. 4 is used. This model consists of 35 discrete levels including the ground state. For a nitrogen molecule and molecular ion, the structure of an energy level contains numerous rotational and vibrational levels in each electronic level. However, if it is asumed that population distributions are determined by rotational temperature (which is substantially equal to heavy-particle translational temperature) for the rotational levels and by vibrational temperature for the vibrational levels, the molecular transfer calculation is limited only to that of electronic levels. In the present study, four electronic states for the molecule are taken into account, that is, $X^1\Sigma_g$ (ground state, electronic excitation energy =0 eV), $A^3\Sigma_u$ (6.17 eV), $B^3\Pi_g$ (8.55 eV), and $C^3\Pi_u$ (11.03 eV) states, and two states for the molecular ion, $X^2\Sigma_g$ (0 eV) and $B^2\Sigma_u$ (3.17 eV) states. From the B state of N_2 molecule, the first positive bands radiation emanates and from the C state, the second positive band radiation. From the B state of N_2^+ ion, the first negative band radiation is emitted.

The rate coefficients for the atomic excitations from the state i to j by an electron impact are taken from Park [4]. The other rate coefficients, that is, those by an heavy-particle impact, the rate coefficient for radiative recombination from the continuum to the state i, and the ionization rate constants by collisions with free elctrons and heavy-particles, are all adopted from Drawin [5, 6].

For the molecular and molecular ion processes, the collisional excitation rate coefficient by an electron impact is given by a sum over all final upper vibrational states and rotational states and an average over all initial lower vibrational states and rotational states. An expression based on such a difinition is given in Refs. 7 and 8. For the electronic excitation rate by the collision with heavy particles, we have no reliable expression. The excitation cross section of any neutral species is known to be zero at the threshold and behaves approximately as

$$Q_{ij}=\sigma \ln (E/E_{ex})/(E/E_{ex}), \tag{6}$$

where σ is a constant and assumed to be 10^{-16} cm^2 according to Park [9]. For the ionic molecule, the excitation cross section is assumed to be

$$Q_{ij}=10^{-17}\ \text{cm}^2, \tag{7}$$

because the cross section value may be nearly constant near the threshold energy as that for an electron impact [10]. In case of the molecular and molecular ionic excitations, the contributions of vibrational and rotational states are neglected because of a large uncertainty in those cross sections and relative unimportance as compared with the electron impact processes. The rate coefficients are simply calculated by Eq. (2) with Eqs. (6) and (7) for the cross sections and with Maxwell

energy distribution for $F(E)$.

4. Results and Discussion

Calculations of the populations at the excited states of a nitrogen atom, nitrogen molecule, and nitrogen molecular ion are conducted for the conditions similar to those in a shock layer over an aero-braked AOTV [1]. Park [11] made a detailed calculation of the shock tube flow for air with a strong shock wave simulating flow properties in the AOTV shock layer. His calculations are based on the simple two-temperature model and contains somewhat inadequate dissociation rate model of a diatomic molecule under thermal nonequilibrium. Nevertheless, the present sample calculations are made based on his flow calculations, bacause no exact fluid dynamical solution has been presented so far for the shock layer region.

Temperature and pressure histories behind a shock wave calculated by Park [11] are reproduced in Fig. 1. This was calculated under the conditions of initial pressure $P=0.1$ Torr and shock Mach number $M=30$. The present calculations on nonequilibrium populations are made for the three points (a), (b), and (c) indicated in the figure. The point (a) typifies the condition in the extremely thermal and chemical nonequilibrium in the relaxation zone behind the shock wave, the point (b) the condition shortly after the peak vibrational (electron) temperature, and the point (c) the near-equilibrium condition. The plasma parameters and the population density of each species are given in Ref. 11, in detail.

Figure 2 shows the distributions of the population density per unit statistical weight at the various electronic states of a nitrogen atom, plotted as a function of the excitation energy from the ground state. Population densities for the Saha equilibrium

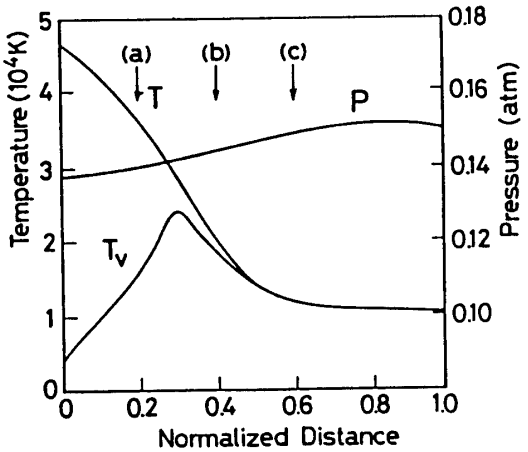

Fig. 1. Temperature and Pressure Histories behind Shock Wave of M=30 and P=0.1 Torr. (The abscissa is normalized by 0.5 cm. See Ref.11.)

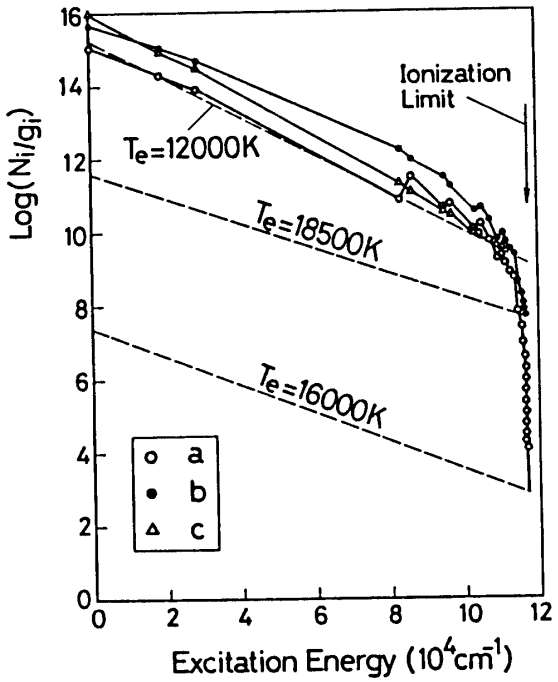

Fig. 2. Population Distributions for N atom.

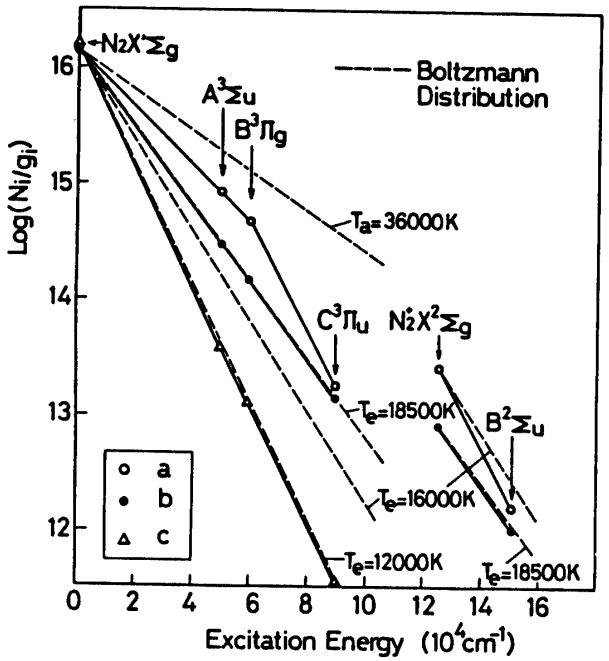

Fig. 3. Population Distributions for N_2 Molecule and N^+_2 Ionic Molecule.

with free electron are also shown by the broken lines, each marked with the corresponding electron temperature. The calculated nonequilibrium populations at the points (a) and (b) are much larger in magnitude than the equilibrium ones for almost all the excited states. The populations just below the inonization limit decrease rapidly as the excitation energy increases owing to the effect of prompt inonization from higher excited states, and approach the equilibrium populations. Such a overpopulation causes radiation enhancement due to atomic processes. It should be noted that, in spite of the extremely nonequilibrium populations, the slopes of the distributions in the main region are almost the same as the equilibrium ones on the whole, that is, the populatiion distributions are governed by the electron temperature at the corresponding point. On the contrary, the point (c) is fairly near to the equilibrium condition due to abundant free electrons. The transitions by heavy particle collisions are practically negligible for all of the points considered.

In Fig. 3, the population density distributions for the nitrogen molecule and nitrogen ionic molecule are plotted against the excitation energy. It is seen that the distribution for the molecule at the point (a) does not coincide with both of the distributions equilibrated with free electrons and heavy particles (broken lines marked with T_e=16,000 K and with T_a=36,000 K, respectively). However, the distributions at the other points agree well with the corresponding equilibrium distributions with free electrons, because the excitation and deexcitation processes by electron impacts are predominant over those by heavy particle impacts. For the point (a), the populations at the $C^3\Pi_u$ state of the nitrogen molecule and the $B^2\Sigma_u$ state of the nitrogen molecular ion are relatively lower than those at the other states. This is because that those states emit the second positive bands and the first negative bands, respectively, at large radiative transition probalibities. Electronic excitation tempera-

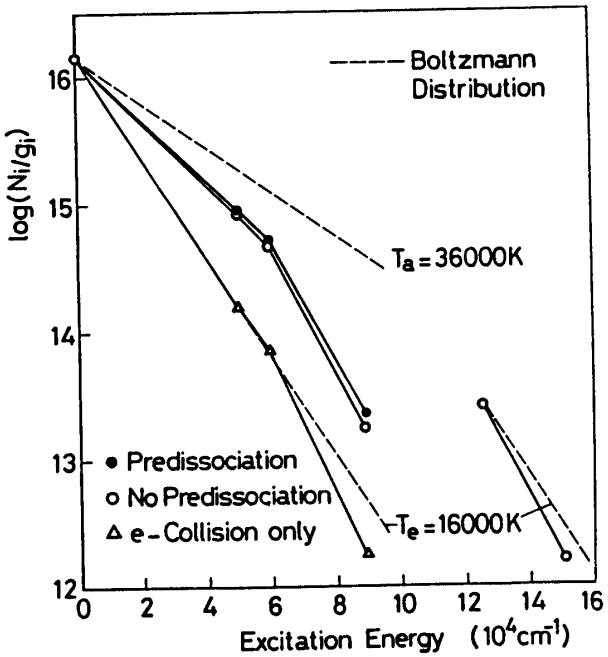

Fig. 4. Effects of Predissociation Process and Heavy Particle Collisions.

ture calculatd from the populations of the ground state and the A or B state is about 24,000 K but that from the populations of the B and C states is about 13,000 K, which is fairly lower than the electron temperature. It should be noted that this figure does not show the strict population distributions at the various electronic states because the total population which distributes over all vibrational and rotaional states is concentrated to the lowest vibrational state of each electronic state. It is understood from this figure that nonequilibrium enhancement of molecular radiation occurs at the early stage of the ralxation zone.

Figure 4 shows comparison of the distribution calculated at the point (a) (termed no predissociation in the figure) with that including the effect of predissociation and inverse-predissociation for the $C^3\Pi_u$ state (termed predissociation) and that excluding the effect of all the heavy particle processes (termed e-collision only). The C state lies above the dissociation limit of a nitrogen molecule (=9.76 eV). Therefore, it may be significantly populated by the collisions between the two atoms through the inverse-predissociation and depopulated by the predissociation. The inverse-predissociation rate is calculated by multiplying the elastic collision frequency by the Boltzmann factor based on the energy difference between the C state and the atomic state with the assumption of the probability factor of unity. The predissociation rate can be deduced by applying the principle of detailed balance. It is found that for the plasma conditions considered, the effect of the predissociation is not so large, but that of the heavy-particle impacts may be significant in the early stage of the relaxation. The effect of the heavy particle impacts for the molecular ion process is negligibly small because the electronic excitation cross section by an electron impact is so large, as compared with that by the heavy particles. If the excitation by the heavy particle collisions is neglected in the calculation, the populations at excited states and hence

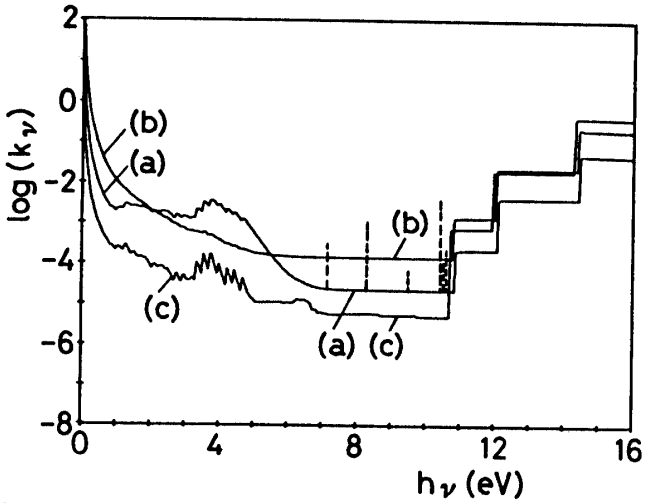

Fig. 5. Absorption Coefficient (in cm^{-1}) vs. Photon Energy.

molecular radiation may be underpredicted, at least, at the very early stage of the relaxation even under the condition of the AOTV flight.

Based on the results of the population density in Figs. 2 and 3, absorption coefficient of the nitrogen plasmas is calculated approximately. In the calculations, the following transitions are taken into account. (1) N_2 first positive bands (v'=0–8, v''0040–9), (2) N_2 second positive bands (v'=0–4, v''=0–10), (3) N_2 Vegard-Kaplan bands (v'=0–8, v''=0–9), (4) N^+_2 first negative bands (v'=0–4, v''=0–5), (5) the bound-bound transitions of N atoms, (6) the bound-free transitons of N atoms, and (7) the free-free transitions of N atoms. Here, v' indicates the upper vibrational quantum number and v'' the lower vibrational quantum number. The contributions of the molecular bands and molecular ion bands are calculated by the smeared rotational line model [12] modified to include the effect of the thermal and chemical nonequilibrium. The atomic bound-bound transitions are claculated with the atomic parameters in Ref. 13. The atomic bound-free and free-free transitions are calculated by the approximate method by Biberman [14], in which the photo-ionization cross section is taken from Ref. 15, and slightly modified to agree better with experiments [16].

Figure 5 shows the absorption coefficient kv (in cm^{-1}) at the three points in Fig. 1 as a function of the photon energy. Several broken lines in the region of hv=7 to 11 eV indicate the absorption by the bound-bound transitions at the point (a). Then, it is assumed that the lines caused by the transitions have Doppler-broadened profile. It is seen from the figure that the absorption by the atomic processes are predominant over that by molecular bands. The contributions from the molecular processes are desplayed in the figure by the rugged curves in the energy range of photon hv=1–5 eV. The plasmas considered here satisfy the condition of $kv \ll 1$, that is, the plasmas are optically thin in almost all the energy range with exception in the very low and very high energy regions.

Figure 6 shows emittance of the plasmas with assumed thickness of 1 cm. The broken lines indicate the atomic lines. It is seen that, in the radiation calculations, the

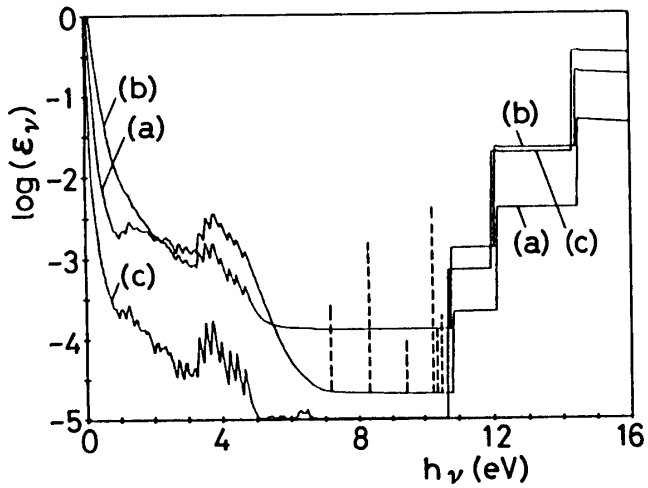

Fig. 6. Emittance vs. Photon Energy.

Vegard-Kaplan bands which appear in the energy region of $h\nu$=5 to 7 eV, are negligible. Theoretically, the emissions with energy of $h\nu \lesssim 5$ eV and $h\nu \gtrsim 11$ eV are mainly responsible for the radiative heating to the vehicle. However, in the real flight, the radiation with the higher energy is not so large as expected, because that can be considerably absorbed by a boundary layer developing over the vehicle.

5. Conclusions

The main conclusions are drawn from the above sample calculations as follows.
(1) The population densities at the electronic states of a nitrogen atom are much larger in magnitude than the equilibrium ones in the early stage of the relaxation region. In spite of it, the distributions themselves among the main states are approximately determined by electron temperature. The effects of the heavy particle impacts on the distributions are negligibly small.
(2) The population distributions at the electronic states of a nitrogen molecule show the nonequilibrium characteristics in the very early stage of the relaxation region. In addition, the heavy particle collisions have significant effect on the nonequilibrium populations. The effect of the predissociation and inverse-predissociation processes seems small.
(3) The emissions with $h\nu \lesssim 5$ eV and $h\nu \gtrsim 11$ eV are mainly responsible for the radiative heating to the vehicle. The plasmas are optically thin for the almost entire photon energy range considered. The absorption characteristics of the plasmas are largely governed by the atomic processes.

References

[1] Menees, G. P., Park, C., and Wilson, J. F.: Design and Performance Analysis of a Conical-Aerobrake Orbital -Transfer Vehicle Concept, AIAA Paper 84-0410, 1984.
[2] Park, C.: Radiation Enhancement by Nonequilibrium in Earth's Atmosphere, AIAA Paper 83-0410, 1983.

[3] Bates, D. R., Kingston, A. E., and McWhirter, R.W.P.: Recombination between Electrons and Atomic Ions, I. Optically Thin Plasmas, Proc. R. Soc., Vol. A267, 1962, pp. 297–312.
[4] Park, C.: Comparison of Electron and Electronic Temperatures in Recombining Nozzle Flow of Ionized Nitrogen-Hydrogen Mixture, Part 1. Theory, J. Plasma Phys., Vol. 9, 1973, pp. 187–215.
[5] Drawin, H. W.: Influence of Atom-Atom Collisions on the Collisional-Radiative Ionization and Recombination Coefficients of Hydrogen Plasmas, Z. Phys., Vol. 225, 1969, pp. 483–493.
[6] Drawin, H. W. and Emard, F.: Influence of Atom-Atom Collisions on the Collisional-Radiative Ionization and Recombination Coefficients of Helium Plasmas, Z. Phys., Vol. 254, 1972, pp. 202–217.
[7] Park, C.: Calculation of Nonequilibrium Radiation in AOTV Flight Regimes, AIAA Paper 84–0306, 1984.
[8] Shirai, H. and Tabei, K.: Non-Maxwell Electron Energy Distribution and Radiation of Nonequilibrium Nitrogen Plasmas, Trans, Jpn. Soc. Aero. Space Sci., Vol. 29, 1986, pp. 89–100.
[9] Park, C.: Assessment of Two-Temperature Kinetic Model for Dissociating and Weakly-Ionizing Nitrogen, AIAA Paper 86–1347, 1986.
[10] Crandall, D. H., Kauppila, W. E., Phaneuf, R. A., Taylor, P. O. and Dunn, G. H.: Absolute Cross Sections for Electron-Impact Excitation of N_2^+, Phys. Rev. A, Vol. 9, 1974, pp. 2545–2551.
[11] Park, C.: On Convergence of Computation of Chemically Reacting Flows, AIAA Paper 85–0247, 1985.
[12] Patch, R. W., Shackleford, W. L. and Penner, S. S.: Approximate Spectral Absorption Coefficient Calculations for Electronic Band Systems Belonging to Diatomic Molecules, J. Quant. Spectrosc. Radiat. Transfer, Vol. 2, 1962, pp. 263–271.
[13] Wiese, W. L., Smith, M. W. and Miles, B. W.: Atomic Transition Probabilities, NBS 22, Washington, D. C., 1969.
[14] Biberman, L. M. and Norman, G. E.: Recombination Radiation and Brehmstralung of a Plasma, J. Quant. Spectrosc. Radiat. Transfer, Vol. 3, 1963, pp. 221–245 (in Russian).
[15] Barfield, W. D., Koontz, G. D. and Huebner, W. F.: Fits to New Calculations of Photoionization Cross Sections for Low-Z Elements, J. Quant. Spectrosc. Radiat. Transfer, Vol. 12, 1972, pp. 1409–1433.
[16] Marrone, P. V. and Wurster, W. H.: Measurements of Atomic Nitrogen and Carbon Photoionization Cross Sections Using Shock Tube Vacuum Ultraviolet Spectroscopy, J. Quant. Spectrosc. Radiat. Transfer, Vol. 11, 1971, pp. 327–348.